Tetrahedron Letters 58 (2017) 365–370

Contents lists available at ScienceDirect

Tetrahedron Letters

journal homepage: www.elsevier.com/locate/tetlet

A Schiff base fluorescence probe for highly selective turn-on recognition of Zn^{2+}

Jinli Zhu [a], Yuhuan Zhang [b], Yihan Chen [a], Tongming Sun [a], Yanfeng Tang [a,*], Yang Huang [b], Qingqing Yang [a], Danyang Ma [a], Yipu Wang [a], Miao Wang [a,*]

[a] School of Chemistry and Chemical Engineering, Nantong University, Nantong 226019, PR China
[b] School of Textiles, Nantong University, Nantong 226019, PR China

ARTICLE INFO

Article history:
Received 10 November 2016
Revised 13 December 2016
Accepted 16 December 2016
Available online 19 December 2016

Keywords:
Zn^{2+} detection
Schiff base
Turn-on fluorescence
Live cells

ABSTRACT

A simple Schiff base **CTS**, synthesized between 2-hydroxy-1-naphthaldehyde and 2-benzylthio-ethanamine, was found to be a good turn-on fluorescence probe for the detection of Zn^{2+}, due to the restriction of the rotation of the bond between C=N and naphthalene ring and/or the blocking of the photo-induced electron transfer (PET) mechanism of the nitrogen atom to naphthalene ring. Excellent selectivity for Zn^{2+} was evidenced, over many other competing ions, including Fe^{3+}, Cr^{3+}, Ni^{2+}, Co^{2+}, Fe^{2+},Mn^{2+}, Ca^{2+}, Hg^{2+}, Pb^{2+}, Cu^{2+}, Mg^{2+}, Ba^{2+}, Cd^{2+}, Ag^{+}, Li^{+}, K^{+}, and Na^{+}, in EtOH/HEPES buffer (95:5, v/v, pH = 7.4). It was noteworthy that Cd^{2+} had no interference with Zn^{2+}. The stoichiometric complex of **CTS**-Zn^{2+} was determined to be 2:1 for **CTS** and Zn^{2+} in molar, based on the Job plot and single crystal X-ray diffraction data. The binding constant of the complex was 85.7 M^{-2} with a detection limit of 5.03×10^{-7} M. The fluorescence bio-imaging capability of **CTS** to detect Zn^{2+} in live cells was also studied. These results indicated that **CTS** could serve as a favorable probe for Zn^{2+}.

Introduction

Currently, a number of metal ions have been verified to be crucial in living organisms, playing irreplaceable roles in a variety of physiological and biochemical processes.[1–4] Among them, Zn^{2+}, the second most abundant metal ion in the human body, likewise participates in many biochemical and physiological processes such as: metabolism of DNA,[5] gene expression,[6] signal transduction,[7] immune function,[8] etc. Modern medical research shows that the imbalance of Zn^{2+} in human bodies can result in numerous serious diseases, including diabetes types I and II,[9] neural dysfunction,[10] Alzheimer,[11] and even certain cancers.[12] Therefore, a method to sensitively and selectively detect Zn^{2+} is of great importance, not only in living systems, but also in environmental waters. Consequently, several detection methods, including atomic absorption spectrometry (AAS),[13] atomic emission spectrometry (AES),[14] voltammetry,[15] electrochemical method,[16] and fluorescent sensors,[17–19] have been developed. Among these various methods, fluorescence chemosensors that detect Zn^{2+} have attracted enormous interest because of their high sensitivity, good selectivity, simplicity and quick-response abilities. To date, most reported fluorescence chemosensors for Zn^{2+} detection have been designed based on quinolone,[20–22] anthracene,[23,24] coumarin,[25,26] BODIPY,[27,28] and fluorescein fluorophores.[29,30] They exhibited good performance for the detection of Zn^{2+}. However, some of them require a complicated synthesis protocol. Most of them suffer from the interference of Cd^{2+} with Zn^{2+}. In this regard, developing an easily prepared, highly sensitive, and excellently selective fluorescence sensor for recognizing Zn^{2+} still remains a challenge.

Taking this into account, Sinha et al., synthesized a series of cysteamine-based fluorescence sensors for Zn^{2+} in pure DMF.[31] In this study, a sensor synthesized between 2-hydroxy-1-naphthaldehyde and 2-benzylthio-ethanamine (Scheme 1) could not detect Zn^{2+} in DMF. However, by coincidence, this compound (abbreviated as **CTS**) was an excellent Zn^{2+} sensor with a detection limit of 5.03×10^{-7} M in EtOH/HEPES buffer (95:5, v/v, pH = 7.4), while Cd^{2+} had no interference with Zn^{2+}. We also obtained a single crystal of the complex of CTS with Zn^{2+}. Moreover, **CTS** has the potential use of detecting Zn^{2+} in living cells.

Results and discussion

Fig. 1 showed the UV–Vis spectra of **CTS** in EtOH/HEPES buffer (95: 5, v/v, pH 7.4). It displayed two weak absorption peaks at 204 nm and 232 nm. Upon the gradual addition of Zn^{2+}, the

* Corresponding authors.
E-mail address: tangyf@ntu.edu.cn (Y. Tang).

http://dx.doi.org/10.1016/j.tetlet.2016.12.041
0040-4039/

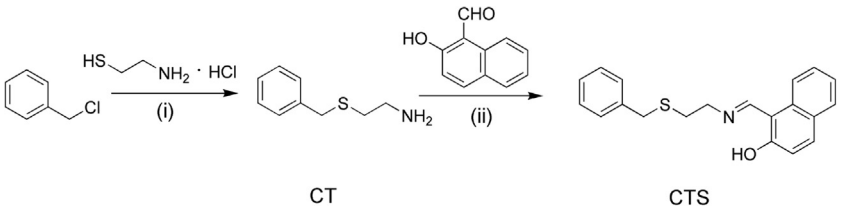

Scheme 1. Synthesis of CTS. (i) NaH, dioxane, 50 °C; (ii) ethanol, reflux.

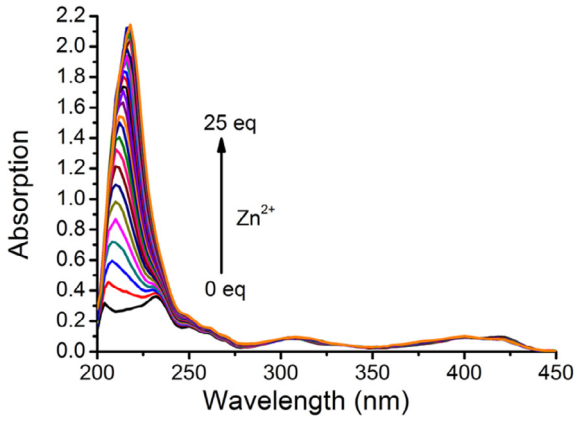

Fig. 1. UV–Vis absorption spectra of **CTS** solution (10 μM, EtOH/HEPES, 95:5, v/v, pH 7.4) upon the addition of different amounts of Zn^{2+} (0–25 equivalents).

absorption peak at 204 nm slightly red-shifted to 218 nm with increasing absorption intensities, and the absorption peak at 232 nm disappeared gradually. These changes, to some extent, indicated the coordinated interaction between Zn^{2+} and **CTS**.

To further corroborate the selective complexation of **CTS** with Zn^{2+}, the fluorescence response behavior of **CTS** to various metal ions was systematically investigated in EtOH/HEPES buffer (95:5, v/v, pH 7.4) (Fig. 2A). Pure **CTS** solution (10 μM) exhibited hardly detectable fluorescence emission at 450 nm at excitation of 242 nm. Upon the addition of Zn^{2+} (100 μM), a significant fluorescence enhancement (19-fold) at 450 nm was observed, demonstrating a Zn^{2+}-selective "off-on" fluorescent signaling behavior of **CTS**. This enhancement directly indicated that the complex of **CTS** with Zn^{2+} was formed. As expected, there was no obvious change in the fluorescence intensity after adding other metal ions to the **CTS** solution, including Fe^{3+}, Cr^{3+}, Mn^{2+}, Hg^{2+}, Pb^{2+}, Cu^{2+}, Ba^{2+}, Cd^{2+}, Al^{3+}, Ni^{2+}, Co^{2+}, Fe^{2+}, Ca^{2+}, Mg^{2+}, Ag^{+}, Li^{+}, K^{+}, and Na^{+} (100 μM) (Fig. S5). To further display that the selectivity was not affected by the metal ions concentrations, the fluorescence intensities of **CTS** added with these metal ions at different concentrations were investigated (Fig. S6). It was clearly seen that the fluorescence intensities of **CTS** were only sensitive to the concentration of Zn^{2+}. It is worth mentioning that there was no interference of Cd^{2+} with Zn^{2+}. Among these **CTS** solutions excited at 254 nm after addition of the certain metal ion, only the solution containing Zn^{2+} exhibited a noticeable color change from green to fluorescent blue, which was easily observed by the naked-eye (Fig. S7). In addition, the fluorescence intensity of **CTS** at different concentrations were investigated. As shown in Fig. S8, the fluorescence intensity of **CTS** decreased with increasing of its concentration, suggesting that

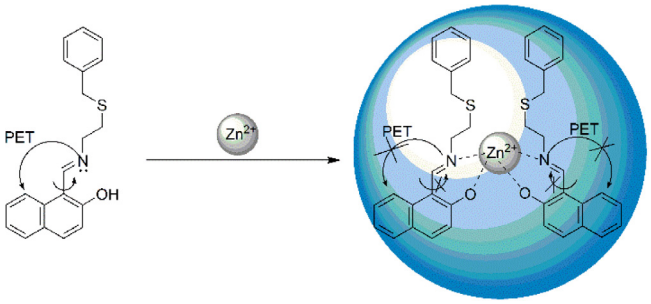

Scheme 2. Proposed binding mechanism between **CTS** and Zn^{2+}.

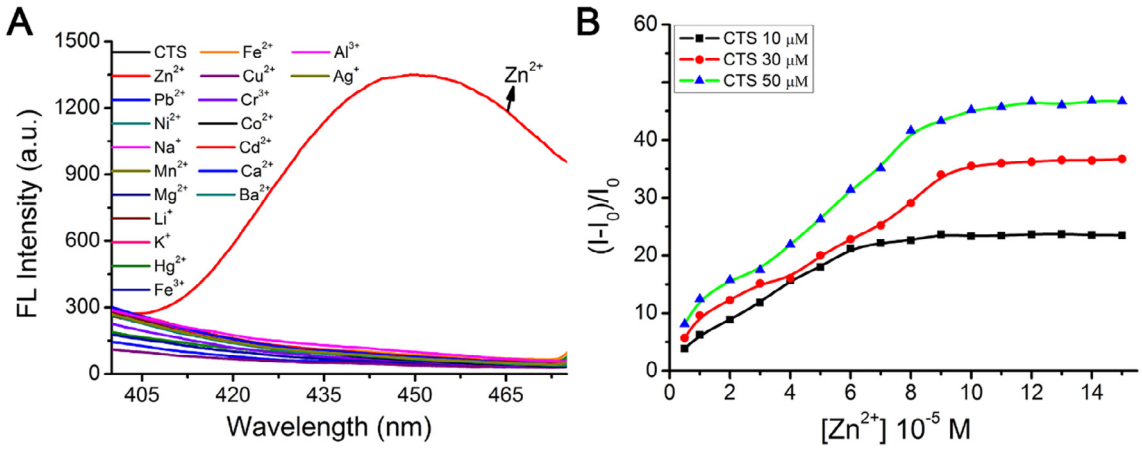

Fig. 2. (A) Fluorescence spectra of **CTS** (10 μM) upon the addition of various metal ions (100 μM) in EtOH/HEPES buffer (95:5, v/v, pH 7.4) at 450 nm. λ_{ex} = 242 nm. (B) The fluorescence intensity multiple changes of **CTS** (10, 30, 50 μM) versus the concentrations of Zn^{2+} (5, 10, 20, 30, 40, 50, 60, 70, 80, 90, 100, 110, 120, 130, 140, 150 μM) in EtOH/HEPES buffer (95:5, v/v, pH 7.4) with the excitation at 242 nm and the emission at 450 nm. I stands for the fluorescence intensity of **CTS** solution sample (10, 30, 50 μM) upon addition of different amount of Zn^{2+} (5, 10, 20, 30, 40, 50, 60, 70, 80, 90, 100, 110, 120, 130, 140, 150 μM); I_0 stands for the fluorescence intensity of pure **CTS** (10, 30, 50 μM) solution without Zn^{2+}.

CTS has the aggregation-caused quenching (ACQ) property.[32,33] The higher concentration of CTS used, the higher times of fluorescence enhancement in the presence of given was observed (Fig. 2B). This result indicated that the binding of Zn^{2+} to **CTS** could induce the disaggregation of **CTS** to further produce turn-on fluorescence response. Compared with DMF in which **CTS** shows no response to Zn^{2+}, the EtOH/HEPES buffer is an ideal sensing condition for Zn^{2+}. The binding of **CTS** with Zn^{2+} formed a rigid framework inhibiting the rotation of the bond between C=N group and naphthalene ring. And at the same time the photoinduced electron transfer (PET) process was blocked and **CTS** was disaggregated after complexation of N with Zn^{2+}. These cooperative interactions are presumed to trigger the turn-on fluorescence response. These three main reasons could be employed to explain this fluorescence enhancement (Scheme 2).[34,35]

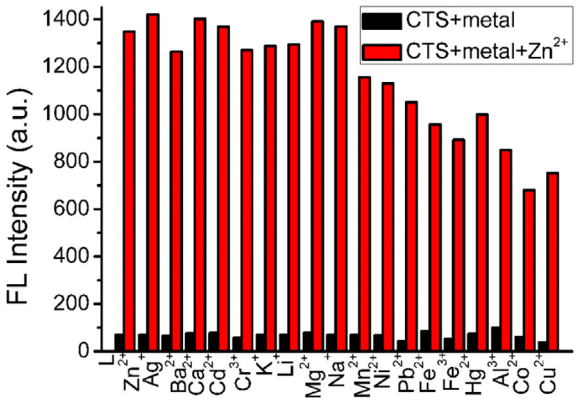

Fig. 3. Fluorescence intensities of **CTS** (10 μM) upon addition of various metal ions (100 μM) (Zn^{2+}, Al^{3+}, Ag^{+}, Cd^{2+}, Co^{2+}, Li^{+}, Mn^{2+}, Na^{+}, Pb^{2+}, K^{+}, Ca^{2+}, Mg^{2+}, Ba^{2+}, Cr^{3+}, Cu^{2+}, Fe^{2+}, Fe^{3+}, Hg^{2+}, Ni^{2+}) and that of the respective solution added Zn^{2+} (100 μM). EtOH/HEPES buffer (95:5, v/v, pH 7.4), λ_{em} = 450 nm, λ_{ex} = 242 nm.

The competitive experiments were carried out to further confirm the unique selectivity of **CTS** to Zn^{2+}. As shown in Fig. 3, it was clear that the fluorescence intensities at 450 nm of the **CTS**-Zn^{2+} solutions did not significantly change after the addition of any one of following metal ions: Ag^{+}, Ba^{2+}, Ca^{2+}, Cd^{2+}, Cr^{3+}, K^{+}, Li^{+}, Mg^{2+}, and Na^{+}. Moreover, it was exciting that there were no interferences of Cd^{2+} and Cr^{3+} with Zn^{2+} due to the highly selective coordination sites of **CTS** for Zn^{2+}. In another case, after the addition of other metal ions, such as Mn^{2+}, Ni^{2+}, Pb^{2+}, Fe^{2+}, Fe^{3+}, Hg^{2+}, Al^{3+}, Co^{2+}, and Cu^{2+}, the fluorescence intensities decreased to some degree compared to that of the **CTS**-Zn^{2+} solution. However, they still displayed strong turn-on signals for the recognition of Zn^{2+}. Therefore, **CTS** had an excellent selectivity for Zn^{2+} in the presence of other competing metal ions.

To further understand the detecting properties of **CTS**, its fluorescence titration was carried out by increasing the concentration of Zn^{2+}. As calculated from the fluorescence titration spectra shown in Fig. 4A, the fluorescence quantum yield of **CTS** increased from 0.0028 to 0.0595 with increasing Zn^{2+} concentration. A strong linear relationship was obtained using the Benesi–Hildebrand analysis[36–38] of the titration profiles based on a 2:1 binding model (Fig. 4D). The binding stoichiometric ratio of **CTS** to Zn^{2+} was 2:1. The 2:1 binding ratio was also confirmed by Job's plot study

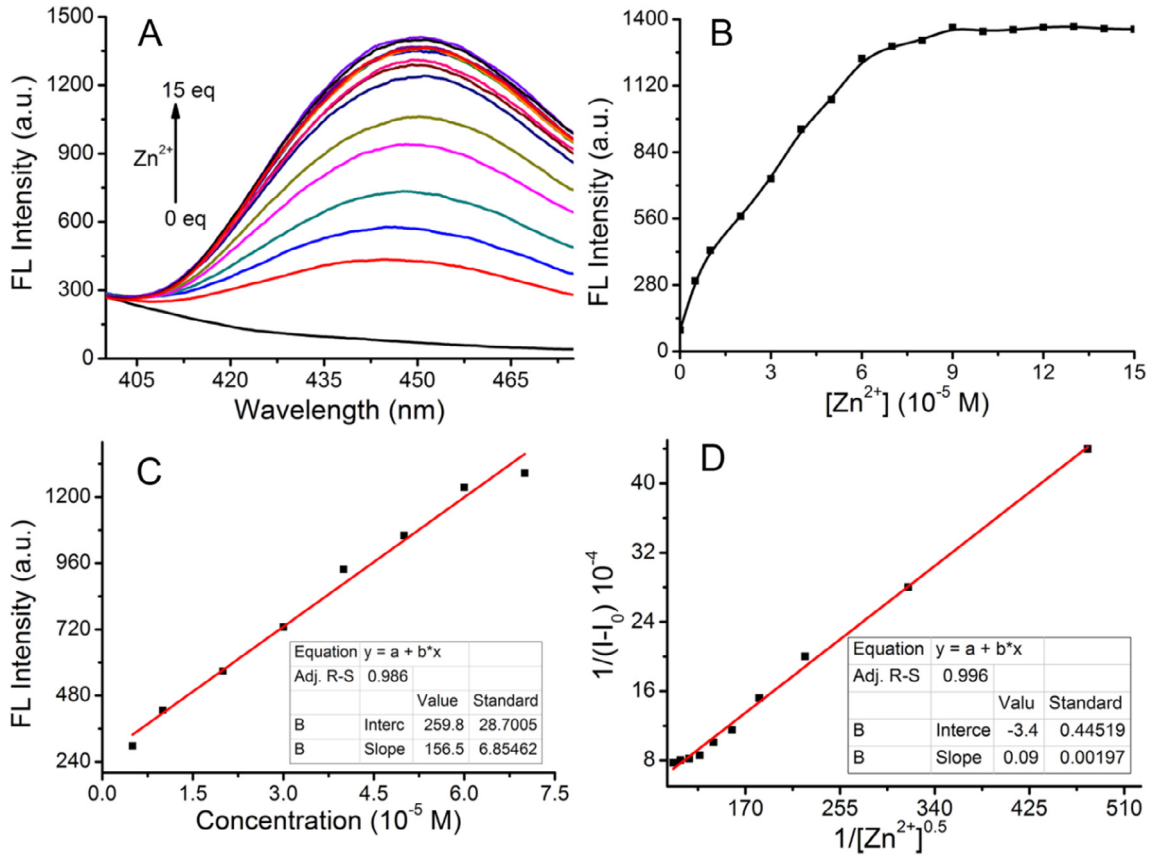

Fig. 4. (A) Fluorescence emission spectra of **CTS** (10 μM) upon the addition of different amount of Zn^{2+}. (B) A plot of fluorescence intensity changes versus the concentrations of Zn^{2+}. (C) Calculation of detection limit of **CTS** (10 μM) for Zn^{2+} (5, 10, 20, 30, 40, 50, 60, 70 μM) . (D) Calculation of binding constant between **CTS** and Zn^{2+}. I stands for the fluorescence intensity of **CTS** solution sample (10 μM) upon addition of different amount of Zn^{2+}; I_0 stands for the fluorescence intensity of pure **CTS** solution. All these data were recorded in EtOH/HEPES buffer (95:5, v/v, pH 7.4) with the excitation at 242 nm and the emission at 450 nm.

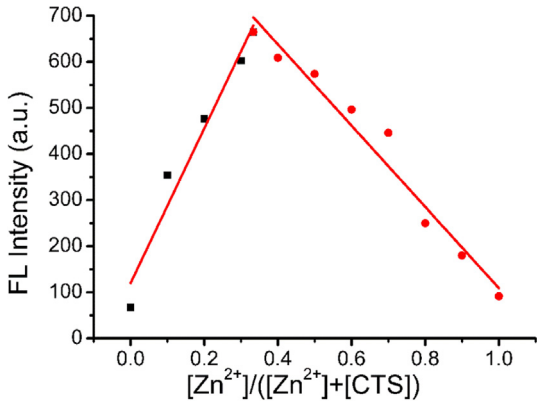

Fig. 5. The Job's plot of fluorescence intensity response of **CTS** to the mole fraction of Zn^{2+} in EtOH/HEPES buffer (95:5, v/v, pH = 7.4), λ_{em} = 450 nm, λ_{ex} = 242 nm.

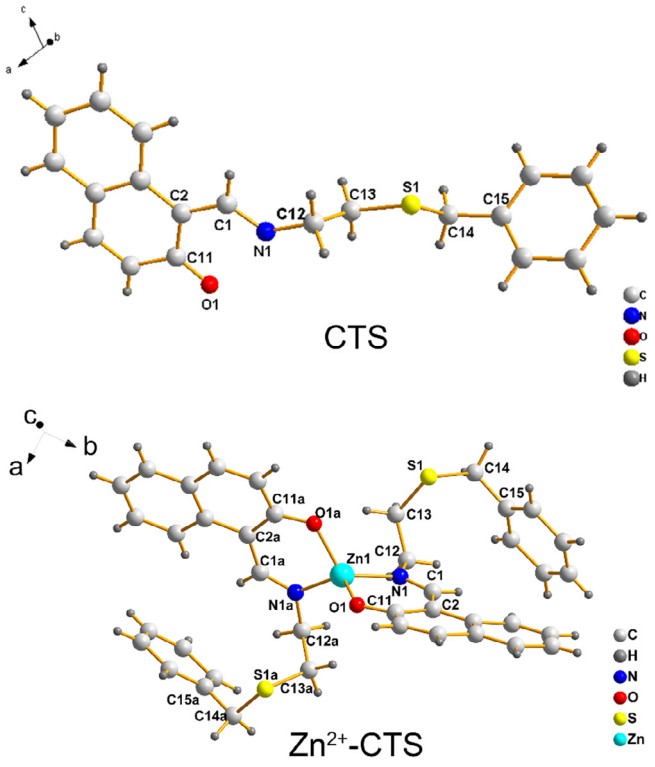

Fig. 6. Crystal structures of CTS–Zn^{2+} and CTS. H atoms were omitted for clarity.

(Fig. 5). In addition, this 2:1 composition of **CTS**-Zn^{2+} complex was further corroborated by the single crystal structure (Fig. 6). Based on the linear relationship shown in Fig. 4C, the detection limit of **CTS** for Zn^{2+} was found to be 5.034×10^{-7} M, which was low enough to detect a submicromolar concentration of Zn^{2+}.

To understand the binding mode of **CTS** with Zn^{2+}, an expected coordination complex was obtained and its structure was shown in Fig. 6. The crystal geometrical parameters of the complex **CTS**-Zn^{2+} and **CTS** were listed in Table S1. The single crystal structure clearly displayed that one Zn^{2+} ion coordinated with two nitrogen atoms and two oxygen atoms of **CTS**, and it was the tetracoordinated metal centre possessing a distorted tetrahedral geometry. The bond distances of Zn—N and Zn—O were in the range of 1.960–1.970 and 1.935–1.945 Å, respectively (Table 1). Upon complexation, some C—N and C—O bond distances in **CTS**-Zn^{2+} changed as shown in Table 2. This crystal structure of **CTS**-Zn^{2+} strongly confirmed that the stoichiometric ratio of **CTS** to Zn^{2+} was 2:1, which

Table 1
Selected bond lengths (Å) and bond angles (°) for compound **CTS** around the Zinc (1) center.

Bond length (Å)			
Zn(1)—O(1)	1.940(5)	Zn(1)—N(1)	1.965(5)
Zn(1)—O(1)a	1.940(5)	Zn(1)—N(1)a	1.965(5)
Bond angles (°)			
O(1)—Zn(1)—N(1)	94.6(2)	O(1)—Zn(1)—O(1)a	104.7(2)
O(1)—Zn(1)—N(1)a	123.8(2)	N(1)—Zn(1)—O(1)a	123.8(2)
N(1)—Zn(1)—N(1)a	117.3(2)	O(1)a—Zn(1)—N(1)a	94.6(2)
C(13)—S(1)—C(14)	102.7(5)	Zn(1)—O(1)—C(11)	125.0(5)
Zn(1)—N(1)—C(1)	124.4(4)	Zn(1)—N(1)—C(12)	118.3(4)

Table 2
Change in bond lengths for **CTS**-Zn^{2+} compared to free **CTS**.

Bond length (Å)	Free ligand (CTS)	Complex (CTS-Zn^{2+})
C(12)—N(1)	1.458(4)	1.487(9)
N(1)—C(1)	1.316(3)	1.290(8)
O(1)—C(11)	1.256(3)	1.294(8)

was consistent with the Job's plot result. Furthermore, it also confirmed what was previously speculated, namely the restriction of bond rotation by the rigid formation of **CTS**-Zn^{2+} and the PET blocking process through the coordination of N with Zn^{2+} after complexation.

For a practical application of **CTS** under physiological conditions, it is necessary to study its pH-stability. As shown in Fig. 7, no noticeable fluorescence emission of pure **CTS** was observed in a wide range of pH values, which suggested that **CTS** can work well under physiological conditions. In the presence of a selective guest like Zn^{2+} ion, the fluorescence intensity of the **CTS**-Zn^{2+} was almost constant in the range of pH 6.0 to 10.0, which clearly indicates the compatibility of **CTS** for biological applications under physiological conditions (Fig. 7). When pH was below 6, the fluorescence intensity of the **CTS**-Zn^{2+} decreased due to the combination of N in imidogen group with H^+.

Before investigating **CTS** acting as a bio-imaging probe, it was necessary to evaluate its cytotoxicity. For this purpose, cultured HeLa cells were incubated with different concentrations of **CTS** (from 0 to 500 μg/mL) for 24 h. Subsequently, MTT assay was carried out according to the reported literature.[39–42] Fig. 8A displayed that, even when treated at a high concentration of **CTS** at 500 μg/mL, over 85% of cells were alive. This result indicates that **CTS** has a low cytotoxicity to cells and is suitable for intracellular imaging.

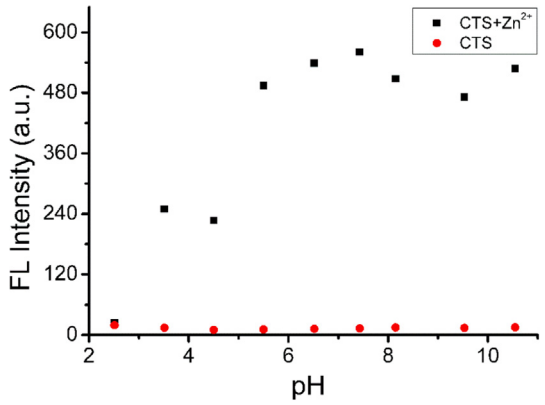

Fig. 7. The fluorescence intensity response of **CTS** (10 μM) and **CTS** with 10 eq of Zn^{2+} to different pH values in Ethanol/H_2O (95:5, V/V), λ_{em} = 450 nm, λ_{ex} = 242 nm.

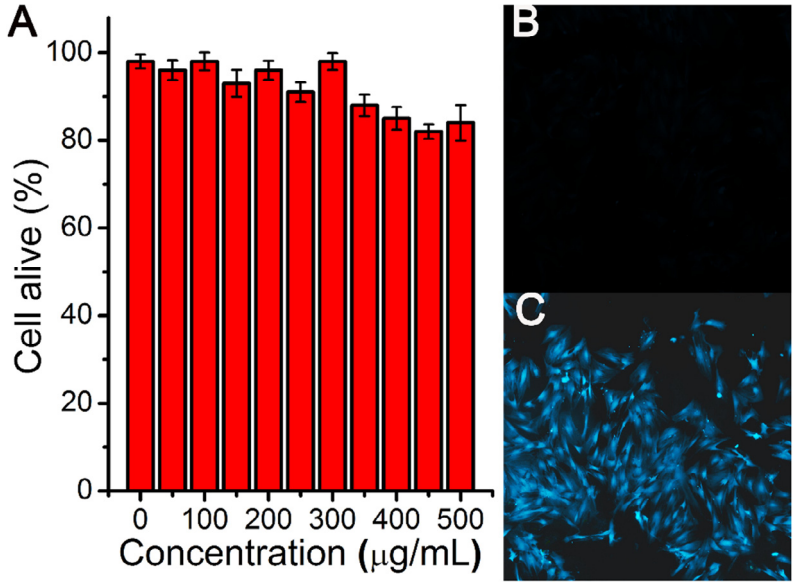

Fig. 8. (A) Cell viability of HeLa cells treated with different concentrations of CTS. Confocal fluorescence micrograph of CTS loaded HeLa cells (B) without and (C) with Zn^{2+}.

Bio-imaging experiments were then performed to study the application of **CTS** to recognize Zn^{2+} in the Hela cells. As illustrated in Fig. 8B, a barely luminescent signal was observed inside the Hela cells only treated with **CTS** in the absence of Zn^{2+}. However, a bright blue fluorescence was observed inside the Hela cells, after pretreating with **CTS** and incubated with Zn^{2+} (1.0 μM, for 15 min) (Fig. 8C). This result provided visual evidence that **CTS** was cell permeable and capable of intracellular detection of Zn^{2+}.

Conclusions

In conclusion, a Schiff base **CTS** was synthesized between 2-hydroxy-1-naphthaldehyde and 2-benzylthio-ethanamine, and was found to be a highly selective fluorescent sensor for the recognition of Zn^{2+} even in the presence of many other metal ions in EtOH/HEPES buffer (95:5, v/v, pH 7.4).This result is different from that tested in DMF depicted in Ref. 31, and the poor performance in DMF may be due to the N atoms in DMF structure inhibiting the coordination. This fluorescence turn-on mechanism can be attributed to three main reasons, namely, hindering rotation of C=N group, PET, and disaggregation of CTS induced by Zn^{2+}- binding. Most notably, **CTS** exhibited no interference of Cd^{2+} to Zn^{2+}. The composition of the complex formed by the coordination of **CTS** with Zn^{2+} was determined to be 2:1 by the Job plot, which was consistent with the analysis of its single crystal structure. The detection limit of **CTS** was estimated to be 5.03×10^{-7} M based on fluorescence titration with a binding constant of 85.7 M^{-2}. Furthermore, biological application of **CTS** was evaluated for the detection of Zn^{2+} in live cells. The results showed that it was of low cytotoxicity and excellent cell membrane permeability, and can recognize the intracellular Zn^{2+}.

Acknowledgements

This work was supported by National Natural Science Foundation of China (No. 21376124, 21476117, 21501100) and Qing Lan Project 2014. We also thanked Analysis and Testing Center of Nantong University for their testing support.

A. Supplementary material

Supplementary data associated with this article can be found, in the online version, at http://dx.doi.org/10.1016/j.tetlet.2016.12.041.

References

1. Komatsu H, Miki T, Citterio D, et al. *J Am Chem Soc*. 2005;127:10798–10799.
2. Tsien RW, Tsien RY. *Annu Rev Cell Biol*. 1990;6:715–760.
3. Farruggia G, Iotti S, Prodi L, et al. *J Am Chem Soc*. 2006;128:344–350.
4. Komatsu H, Iwasawa N, Citterio D, et al. *J Am Chem Soc*. 2004;126:16353–16360.
5. Murcia JM, Molinete M, Gradwohl G, Simonin F, Murcia G. *J Mol Biol*. 1989;210:229–233.
6. Frommer G, Vorbruggen G, Pasca G, Jackle H, Volk T. *EMBO J*. 1996;15:1642–1649.
7. Bouain N, Shahzad Z, Rouached A, et al. *J Exp Bot*. 2014;65:5725–5741.
8. El-Hallag IS. *J Chil Chem Soc*. 2010;55:374–380.
9. Søndergaard LG, Stoltenberg M, Flyvbjerg A, et al. *APMIS*. 2003;111:1147–1154.
10. Hirzel1 K, Müller U, Latal AT, et al. *Neuron*. 2006;52:679–690.
11. Budimir A. *Acta Pharm*. 2011;61:1–14.
12. Prasad AS. *Mol Med*. 2008;14:353–357.
13. Jianrong C, Teo KC. *Anal Chim Acta*. 2001;450:215–222.
14. Monasterios CV, Jones AM, Salin ED. *Anal Chem*. 1986;58:780–785.
15. Van den Berg CMG. *Mar Chem*. 1985;16:121–130.
16. Oliveira PRD, Mendes ACL, Gogola JL, Mangrich AS, Junior LHM, Bergamini MF. *Electrochim Acta*. 2015;151:525–530.
17. Bozym RA, Thompson RB, Stoddart AK, Fierke CA. *ACS Chem Biol*. 2006;1:103–111.
18. Leevy WM, Johnson JR, Lakshmi C, Morris J, Marquez M, Smith BD. *Chem Commun*. 2006;1595–1597.
19. Nolan EM, Jaworski J, Okamoto K-I, Hayashi Y, Sheng M, Lippard SJ. *J Am Chem Soc*. 2005;127:16812–16823.
20. Ponnuvel K, Kumar M, Padmini V. *Sensor Actuat B-Chem*. 2016;227:242–247.
21. Nasir MS, Fahrni CJ, Suhy DA, Kolodsick KJ, Singer CP, O'Halloran TV. *J Biol Inorg Chem*. 1999;4:775–783.
22. Qian WJ, Aspinwall CA, Battiste MA, Kennedy RT. *Anal Chem*. 2000;72:711–717.
23. Xu ZC, Qian XH, Cui JN, Zhang R. *Tetrahedron*. 2006;62:10117–10122.
24. Xu Z, Beak K-H, Kim HN, et al. *J Am Chem Soc*. 2009;132:601–610.
25. Komatsu K, Urano Y, Kojima H, Nagano T. *J Am Chem Soc*. 2007;129:13447–13454.
26. Xu ZC, Liu X, Pan J, Spring DR. *Chem Commun*. 2012;48:4764–4766.
27. Wu YK, Peng XJ, Guo BC, et al. *Org Biomol Chem*. 2005;3:1387–1392.
28. Cao J, Zhao CC, Wang XZ, Zhang YF, Zhu WH. *Chem Commun*. 2012;48:9897–9899.
29. Hirano T, Kikuchi K, Urano Y, Nagano T. *J Am Chem Soc*. 2002;124:6555–6562.
30. Walkup GK, Burdette SC, Lippard SJ, Tsien RY. *J Am Chem Soc*. 2000;122:5644–5645.
31. Sinha S, Dey G, Kumar S, et al. *ACS Appl Mater Interfaces*. 2013;5:11730–11740.

32. Yuning H, Jacky WYL, Ben ZT. *Chem Commun*. 2009;29:4332–4353.
33. Wang ZY, Ping L, Chen Shuming, et al. *Adv Mater*. 2010;22:2159–2163.
34. Yuan M, Li Y, Li J, et al. *Org Lett*. 2007;9:2313–2316.
35. Yuan M, Zhou W, Liu X, et al. *J Org Chem*. 2008;73:5008–5014.
36. Benesi HA, Hildebrand JH. *J Am Chem Soc*. 1949;71:2703–2707.
37. Yannis LL. *J Phys Chem B*. 1997;101:4863–4866.
38. Jisha VS, Thomas AJ, Ramaiah D. *J Org Chem*. 2009;74:6667–6673.
39. Sun J, Yang SW, Wang ZY, et al. *Part Part Syst Char*. 2015;32:434–440.
40. Yang SW, Sun J, He P, et al. *Chem Mater*. 2015;2004:27–67.
41. Zhu C, Yang SW, Wang G, et al. *Mater Chem B*. 2015;3:6871–6876.
42. Yang SW, Sun J, Zhu C, He P, Peng Z, Ding GQ. *Analyst*. 2016;141:1052–1059.